1281. Development of nanostructured Al/SiO2 composite film for vibroisolation applications

Arvydas Palevicius[1], Regita Bendikiene[2], Gediminas Marozas[3], Algirdas Lazauskas[4], Viktoras Grigaliunas[5], Asta Guobiene[6], Egle Fataraite[7]

[1]Department of Mechanical Engineering, Kaunas University of Technology, Kaunas, Lithuania
[2, 3]Department of Manufacturing Engineering, Kaunas University of Technology, Kaunas, Lithuania
[4, 5, 6, 7]Institute of Materials Science, Kaunas University of Technology, Kaunas, Lithuania
[1]Corresponding author
E-mail: [1]*arvydas.palevicius@ktu.lt*, [2]*regita.bendikiene@ktu.lt*, [3]*gediminas.marozas@ktu.lt*, [4]*algirdas.lazauskas@ktu.lt*, [5]*viktoras.grigaliunas@ktu.lt*, [6]*asta.guobiene@ktu.lt*, [7]*egle.fataraite@ktu.lt*

(Received 2 May 2014; received in revised form 13 May 2014; accepted 16 May 2014)

Abstract. This paper presents the investigation of surface morphology, wetting and chemical properties of the nanocomposite Al/SiO_2 film, which can be used as a shock generated vibration isolator for microelectromechanical devices. AFM analysis shows that two-step prepared Al/SiO_2 composite film has regular nanoisland type surface topography provided by SiO_2 nanospheres. EDS analysis confirms that SiO_2 nanospheres are well distributed on the substrate. Carbon found in the composition of composite film can be attributed to the residuals of organic compounds used for the preparation of SiO_2 nanospheres. FTIR analysis confirms formation of the Si-O and Si-OH functional groups and the presence of $–CH_3$ stretching group can be related to the improved non-wetting behavior of the composite.

Keywords: nanospheres, nanostructured, vibration isolation surface.

1. Introduction

Modification of oxide nanostructures and preparation of hybrid composites are constantly being investigated to develop new functional materials with enhanced properties [1]. A mono-dispersed metal coated spheres are ideal to build photonic crystals with large dielectric contrast, which has been demonstrated to have complete photonic band gap [2]. The SiO_2 spheres are widely applied as a catalysts [3] and in biomedical applications [4]. The procedure for generating carbon nanotubes on patterned submicron-size SiO_2 spheres was demonstrated in [5]. The authors concluded that SiO_2 spheres provide a high curvature surface and the growth of carbon nanotubes on such surface gives the nanotubes a novel structure. Glass surfaces coated with modified SiO_2 nanoparticles exhibited excellent superhydrophobic characteristics as it was reported in [6]. By using colloidal self-assembly of nanoparticle spheres in a solvent, it has been possible to prepare more robust composite materials. Ordered nano- or micro-composites were prepared from functionalized SiO_2 nanoparticles by colloidal crystallization in crosslinked resins [7]. Recently, Al/SiO_2 composites were demonstrated to posses many advantageous properties such as low density, high specific strength and good wear resistance [8]. The Al/SiO_2 nanocomposite produced by accumulative roll-bonding process exhibited good tribological properties as tested by pin-on-disc test in [9]. Aluminium matrix composites reinforced with SiO_2 nanoparticles produced via powder metallurgy technique [10] exhibited hardness and tensile strength up to 50 HBR and 323.77 MPa, respectively.

The Al/SiO2 composite film curved-surface structure could reduce the impact force by distributing the contact force over a larger contact area acting as over-range stop protector and shock generated vibration isolator for microelectromechanical devices like gyroscopes, resonators, or oscillators [11]. Thus, Al/SiO_2 composites should be studied in detail with a focus on their structure-property relationship.

In the present study, we demonstrate fabrication of nanostructured Al/SiO_2 composite films on Si(100) substrates via combination of chemical and physical vapour deposition method. A detailed surface characterization of resulting films was conducted by means of atomic force microscopy

(AFM). Energy-dispersive X-ray spectroscopy (EDS) was employed to qualitatively evaluate surface chemical composition and elemental distribution. The wetting characteristics of the nanostructured films were evaluated using contact angle (CA) measurements. Fourier transform infrared spectroscopy (FTIR) was performed to investigate chemical and functional properties of these films.

2. Experimental technique

The SiO_2 nanospheres were prepared by the Stöber method. Briefly, tetraethyl orthosilicate (TEOS) was added to a mixture of ethanol and water solution, followed by the addition of ammonia (28 %). The solution was then stirred for several hours, after which the final solution was spin-coated on a polished Si(100) substrates. Spin speed was ~3000 rpm and spinning time was 30 s. Afterwards, the samples (i.e. SiO_2/Si(100)) were left to dry at room temperature (23 ºC) for 5 hours.

Aluminium thin film deposition on SiO_2/Si(100) was performed using e-beam evaporation technique. Base chamber pressure was maintained using a turbomolecular pump and was $\leq 1 \times 10^{-3}$ Pa. Electron beam gun power was 6 kW and >99 % pure aluminium granules (1 to 4 mm diameter) were used as source material. A final thickness of 30 nm aluminium films was obtained and monitored during the deposition using a quartz crystal monitor. Additionally, aluminium thin films were deposited on Si(100) substrates using the same deposition conditions. The Al/Si(100) samples were used for comparative purpose.

AFM experiments were carried out in air at room temperature using atomic force microscope NT-206 (Microtestmachines Co) and SPM-data processing software SurfaceXplorer. The topographical images were collected using a V-shaped silicon cantilever (spring constant of 3 N/m, tip curvature radius 10.0 nm, cone angle 20º) operating in the contact image mode with a scan size of 544 nm×550 nm. The surface morphology of the resulting films was evaluated based on the AFM surface topography images, height distribution histograms, bearing ratio curves and roughness parameters, including the root mean square roughness (R_q), skewness (R_{sk}) and kurtosis (R_{ku}). The R_q is the average of the measured height deviations taken within the evaluation area and measured from the mean linear surface. The skewness parameter indicates the symmetry of the surface within the evaluation area. A negative R_{sk} indicates a predominance of valleys while a positive R_{sk} value indicates a surface dominated by peaks. Kurtosis is a measure of the height randomness and sharpness of a surface. For a Gaussian-like surface, R_{ku} it has a value of 3. The farther R_{ku} is from 3, the less random and more repetitive is the surface. The height distribution histogram shows the share of surface points located at a given height relative to the total number of surface points in percent. The bearing ratio curve is defined as the dependence of solid material occurrence on feature height.

The qualitative analysis of approximate composition and the elemental map of the Al/SiO_2 film surface, was performed using e_Line plus multi-application nanoengineering workstation (Raith) equipped with a XFlash silicon drift detector (Bruker). No sample coating or any other type of preparation was performed before EDS analysis.

FTIR measurements were carried out for identification of the surface functional groups. A Vertex 70 FTIR spectrometer (Bruker Optics Inc.) equipped with a 30Spec (Pike Technologies) specular reflectance accessory having a fixed 30º angle of incidence (3/16" sampling area mask) was used in this study. The spectrum was recorded in the range of 400-4000 cm^{-1} at a resolution of 4 cm^{-1}. Software OPUS 6.0 (Bruker Optics Inc.) was used for data processing of the baseline-corrected spectra. Reflectance spectra were converted to be displayed as absorbance versus wavelength in cm^{-1}.

Contact angle (CA) measurements were performed at room temperature (23 ºC) using the sessile drop method. One droplet of deionized water (≈2 µl) was deposited onto the pp-HMDSO surface. Optical images of the droplet were obtained and contact angle measured using a method

based on active contours.

3. Results and discussions

Normalized height distribution histograms and bearing ratio curves with their corresponding topographical images of Al/Si(100) control sample and nanostructured Al/SiO_2 composite film are shown in Fig. 1, respectively. The e-beam evaporation of aluminium on Si(100) resulted in smooth surface (R_q: 1.26 nm) with randomly distributed nanostructural features. The random distribution is confirmed by kurtosis parameter, R_{ku} having a value of 3.02. The nanostructural features observed in Fig. 1a$_1$ are in the form of small peaks which dominate (R_{sk}: 1.01) within the evaluation area. The height of the peaks was observed in the range of ~6-8 nm. In contrast, Al/SiO_2 composite film surface shown in Fig. 1b$_1$ has a high curvature distribution provided by SiO_2 spheres. The surface is composed of island-like morphological features, which are separated by deep valley contour indicating leptokurtoic [12] distribution of morphological features with a higher kurtosis value of 3.60. The width of the observed structures was determined to be in the range of ~118-153 nm. The island-like features connect with each other at the height of 9 nm (Fig. 1b). The Al/SiO_2 composite film is considerably rough with R_q value of 6.39 nm. It can be also seen, that SiO_2 nanospheres were well arranged (in a repetitive manner) during the spin-coating procedure.

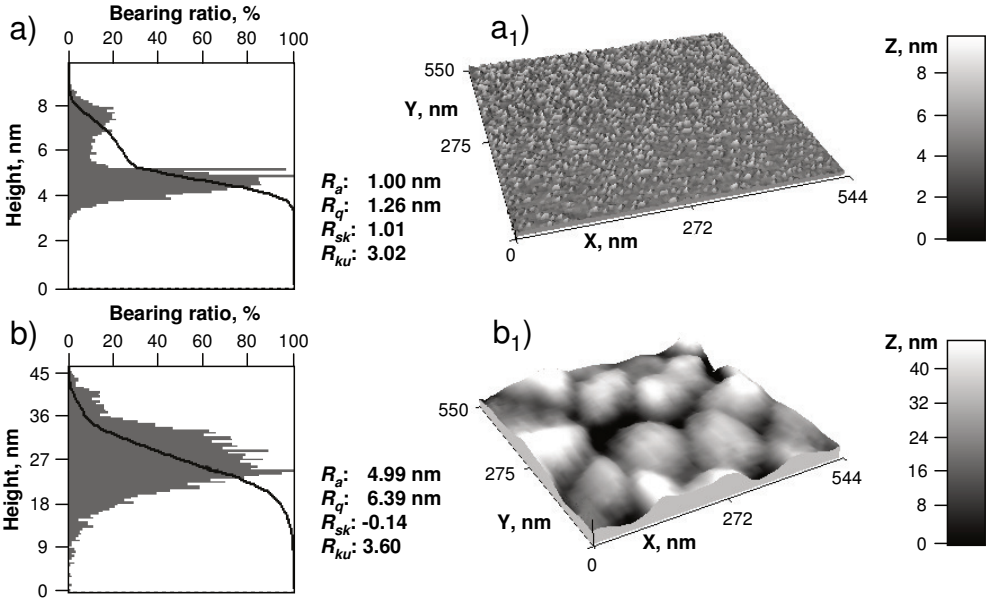

Fig. 1. Normalized height distribution histograms and bearing ratio curves of (a) Al thin film on Si(100) substrate and (b) nanostructured Al/SiO_2 composite film on Si(100) substrate with corresponding AFM topographical images (a$_1$) and (b$_1$) with normalized Z, nm scale and roughness parameters, respectively

The Al/Si(100) control samples exhibited static CA value of 58º. In contrast, nanostructured Al/SiO_2 composite film exhibited better non-wetting properties with the static CA value of 88º. It can be purposed that SiO_2 nanospheres produced a nanostructured surface morphology which reduced the solid fraction that was in contact with the water droplet, thus improving non-wetting properties of the Al/SiO_2 surface.

The EDS spectra of nanostructured Al/SiO_2 composite film on Si(100) substrate with corresponding EDS maps are shown in Fig. 6. The EDS spectra indicates that nanostructured composite film is composed of Si, O, Al and C. It can be proposed that carbon found on the surface could originate from residual ethanol or orthosilicate used for preparation of SiO_2 nanospheres.

The EDS maps of Si and O shown in the (inset) of Fig. 2 confirm that SiO_2 nanospheres were well distributed on the surface of Si(100) substrate. The Al EDS map indicates rather inhomogeneous fashion of the film coverage which is a result of random fluctuation, or noise, that exists naturally during the deposition process as atoms do not arrive at the surface uniformly. Additionally, surface diffusion or shadowing effect could have contributed to such distribution of Al.

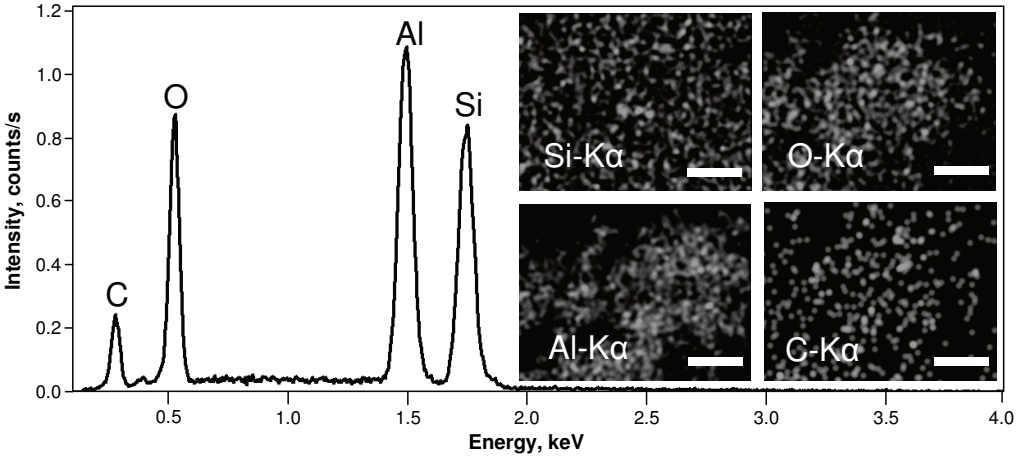

Fig. 2. EDS spectra of nanostructured Al/SiO_2 composite film on Si(100) substrate. An EDS map (inset) is showing the distribution of Si, O, Al and C on the surface of Al/SiO_2 composite film. Mark size 10 μm

Fig. 3 shows panoramic FTIR spectra of Al/Si(100) control sample and nanostructured Al/SiO_2 composite film. In FTIR spectra of Al/Si(100) control sample only substrate (i.e. Si(100)) contributions are visible. The broad band between 3200 and 3700 cm^{-1} can be assigned to O-H stretching in Si-OH bonds [13]. The band assigned to Si-O stretching vibration that appears between 830 and 955 cm^{-1} corresponds to the strongly hydrogen-bonded Si-OH groups [14]. Similarly, these functional groups can be observed in nanostructured Al/SiO_2 composite film.

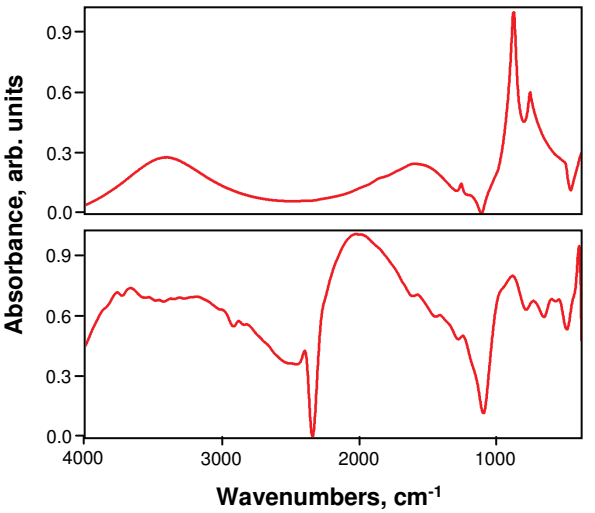

Fig. 3. Panoramic FTIR spectra of (top) Al thin film on Si(100) substrate and (bottom) nanostructured Al/SiO_2 composite film on Si(100) substrate

They can also be present from substrate contribution or SiO_2 nanospheres itself. Additionally, the peak located at 2888 cm^{-1} indicates –CH_3 stretching groups [15], which can be from unreacted

TEOS [15]. Specifically, the methyl groups are associated with a low surface energy [16] and contribute to improved non-wetting characteristics of the resultant composite film. A broad absorption band centered at 2039 cm^{-1} can be assigned to CO adsorbed on the surface [17]. Band at 1592 cm^{-1} is attributed to C=C stretching mode. The evidence of carbon-related functional groups is in good agreement with EDS measurement results.

4. Conclusions

This work has studied the surface morphology, wetting and chemical properties of the Al/SiO_2 composite films. These films were prepared via combination of chemical and physical vapour deposition method. The composite films were characterized using AFM, EDS, FTIR and CA measurements. AFM analysis showed that Al/SiO_2 composite film exhibited island-like morphological features, which were separated by deep valley contour indicating leptokurtoic distribution of morphological features. The nano-structurization of the surface was provided by SiO_2 nanospheres. The composite film showed static water CA with a value of 88º. EDS analysis confirmed that SiO_2 nanospheres were well distributed on the surface of Si(100) substrate. Carbon found in the composition of composite film was attributed residual ethanol or unreacted TEOS used for preparation of SiO_2 nanospheres. FTIR analysis indicated the formation of Si-O and Si-OH functional groups. The presence of $–CH_3$ stretching groups was attributed to improved non-wetting characteristics.

Atomic force microscopy experiments were performed by Algirdas Lazauskas and Asta Guobiene. The energy dispersive X-ray spectroscopy analysis was done by Viktoras Grigaliunas. Fourier transform infrared spectroscopy was performed by Algirdas Lazauskas. Egle Fataraite and Gediminas Marozas contributed to the contact angle measurements and preparation of the nanocomposite film. Arvydas Palevicius and Regita Bendikiene fulfilled the discussion part.

Acknowledgments

This research work was funded by a Grant No. VP1-3.1-ŠMM-08-K-01-015 from Ministry of Education and Science, Lithuania.

References

[1] **Sohn Y.** SiO2 nanospheres modified by Ag nanoparticles: Surface charging and CO oxidation activity. Journal of Molecular Catalysis A: Chemical, Vol. 379, 2013, p. 59-67.

[2] **Zhu M., Qian G., Wang Z., Wang M.** Fabrication of nanoscaled silica layer on the surfaces of submicron SiO2-Ag core-shell spheres. Materials Chemistry and Physics, Vol. 100, Issues 2-3, 2006, p. 333-336.

[3] **Yuan H., Liu H.-Y., Diao J.-Y., Gu X.-M., Su D.-S.** Supported carbon nanotubes on SiO2 spheres as robust monolithic catalysts for the oxidative dehydrogenation of ethylbenzene. New Carbon Materials, Vol. 28, Issue 5, 2013, p. 336-341.

[4] **Flores J. C., Torres V., Popa M., Crespo, D., Calderón-Moreno J. M.** Preparation of core-shell nanospheres of silica-silver: SiO2@Ag. Journal of Non-Crystalline Solids, Vol. 354, Issues 52-54, 2008, p. 5435-5439.

[5] **Huang S.** Growing carbon nanotubes on patterned submicron-size SiO2 spheres. Carbon, Vol. 41, Isseu 12, 2003, p. 2347-2352.

[6] **Lazauskas A., Baltrusaitis J., Grigaliūnas V., Jucius D., Guobienė A., Prosyčevas I., Narmontas P.** Characterization of plasma polymerized hexamethyldisiloxane films prepared by arc discharge. Plasma Chemistry and Plasma Processing, Vol. 34, Issue 2, 2014, p. 271-285.

[7] **Kulkarni S., Wunder S. L.** Moduli of ordered polymer composites prepared by colloidal crystallization of nano- and micro-SiO2 spheres in crosslinked methacrylate resins. Mechanics of Materials, Vol. 43, Issue 11, 2011, p. 643-653.

[8] **Zhu H., Dong K., Huang J., Li J., Wang G., Xie Z.** Reaction mechanism and mechanical properties of an aluminum-based composite fabricated in-situ from Al–SiO2 system. Materials Chemistry and Physics, Vol. 145, Issue 3, 2014, p. 334-341.

[9] **Kadkhodaee M., Moradghol J., Daneshmanesh H., Hashemi B.** Tribological properties of Al/SiO2 nanocomposite sheets produced by accumulative roll bonding (ARB) process. 3rd International Conference on UltraFine Grained and NanoStructured Materials, Tehran, Iran, 2011.

[10] **Ahmed T., Mamat O.** Characterization and properties of aluminium-silica sand nanoparticle composites. Solid State Science and Technology, Vol. 19, Issue 1, 2011, p. 138-149.

[11] **Dong J., Li X., Wang Y., Lu D., Ahat S.** Silicon micromachined high-shock accelerometers with a curved-surface-application structure for over-range stop protection and free-mode-resonance depression. Journal of Micromechanics and Microengineering, Vol. 12, 2002, p. 742-746.

[12] **Gadelmawla E. S., Koura M. M., Maksoud T. M. A., Elewa I. M., Soliman H. H.** Roughness parameters. Journal of Materials Processing Technology, Vol. 123, Issue 1, 2002, p. 133-145.

[13] **Aumaille K., Vallee C., Granier A., Goullet A., Gaboriau F., Turban G.** A comparative study of oxygen/organosilicon plasmas and thin SiOxCyHz films deposited in a helicon reactor. Thin Solid Films, Vol. 359, Issue 2, 2000, p. 188-196.

[14] **Awazu K., Kawazoe H., Seki K.** Growth mechanisms of silica glasses using the liquid phase deposition (LPD). Journal of Non-Crystalline Solids, Vol. 151, Issue 1, 1992, p. 102-108.

[15] **Gomes J., Gomes J.** Comparative study of geometry and bonding character for methoxy radical adsorption on noble metals. Journal of Molecular Structure: Theochem, Vol. 503, Issue 3, 2000, p. 189-200.

[16] **Beganskienė A., Sirutkaitis V., Kurtinaitienė M., Juškėnas R., Kareiva A.** FTIR, TEM and NMR investigations of Stöber silica nanoparticles. Materials Science, Vol. 10, Issue 4, 2004, p. 287-290.

[17] **Guerrero-Ruiz A., Rodriguez-Ramos I.** Spillover and mobility of species on solid surfaces. Elsevier, 2001.